

## FREQUENCY SELECTIVE SURFACES

E.A. Parker, R.J. Langley, R. Cahill and J.C. Vardaxoglou

Electronics Laboratories, The University of Kent, Canterbury, UK

INTRODUCTION

The purpose of this paper is to summarise the performance of four arrays of elements suitable for use as plane dual band frequency selective surfaces in oblique incidence diplexers (Fig.1), capable of giving relatively close band spacings, with centre frequency ratios of about 1.3-1.6. They are characterised by transmission/frequency curves which show two prominent reflection bands, between which is a region of adequate transmission. The centre frequency of at least one of these reflection bands is relatively insensitive to angle or plane of incidence, and is the one normally used in conjunction with the intervening transmission region in dual band operation. Band spacing ratios as small, or even smaller, can of course be achieved by using multiple sheets of capacitive or inductive grids, or of simple resonant elements such as closely packed rings or square loops, which in single layer form give ratios of 3:1 or more. The elements discussed here exchange complexity of array stacking for complexity of element geometry.

ARRAY ELEMENTS

One much studied element suited to this application is the Jerusalem cross (1). Even in its simplest form (Fig.2a), without its inductive grid, where detailed scalar equivalent circuit models are available for design work (2,3), its transmission response approximates to the double resonance structure outlined above. There are, however, minor additional resonances whose origin has been discussed elsewhere (4,5) in terms of the element current distribution. Two other structures with similar frequency responses are the concentric ring (6) and the double square shown in Fig.2c. The spacing of the reflection and transmission bands is determined largely by the spacing of the two resonant frequencies for all three structures. The location of the upper resonance tends to vary with the plane of incidence, which not only restricts the available reflection bandwidth but also, as illustrated below, degrades the crosspolar performance. When, as is often the case, the operating transmission band is required to be below the reflection band in frequency, gridded elements, such as that shown in Fig.2d, provide an alternative to the use of complementary structures. The dimensions of the square largely determine the (upper) reflection band, which is insensitive to angle of incidence when the gap between the grid and the square is small.

ANALYSIS OF CONCENTRIC RING ARRAYS

Concentric rings are not readily represented by a simple LC equivalent circuit, although in design work a first order approximation is to equate the ring circumferences to the resonant wavelengths. An alternative approach is to use the modal technique (7) which has

the advantage of being a vector description but has the disadvantage of requiring substantial computer power. We have expanded the currents (6) in plane ring structures in the form

$$\underline{I} = \sum_{m,n} (a_m \cos ma + b_n \sin na) \hat{\underline{e}} \quad (1)$$

where  $m, n = 0, 1, 2, \dots$  and the position angle  $\alpha$  is defined in Fig.2b.  $\hat{\underline{e}}$  is a unit vector in the direction of increasing  $\alpha$ .

To reduce the computer requirements it is desirable to include as few current modes as is consistent with an adequate fit of the transmission/frequency curves to measurements in test cases. The concentric ring arrays sketched in Fig.2b are resonant in the 10-40 GHz range and are printed on polyester substrates with thicknesses ranging between 0.021 mm and 0.134 mm. Comparison with measured transmission coefficients suggests that the predictions are relatively insensitive to the number of current functions chosen and, for the thinnest substrate, are also insensitive to uncertainties in the value of the dielectric constant. The fit to the measured transmission curves improves asymptotically with the number of Floquet modes (7) used to expand the fields close to the array. Fig.3a shows that the agreement is satisfactory up to about 40 GHz in the E-plane with 169 Floquet modes and only one current function in each ring, corresponding to  $m = 1, n = 0$  in equation (1).

In the H-plane, including terms with  $m = 3$  and 5 in addition to  $m = 1$  reduces the lower resonance by about 0.2 GHz only, for incidence at  $\theta = 45^\circ$ , while the computer CPU time requirement rises by a factor of about 11. With the substrate 0.134 mm thick, the predicted resonant frequencies depend on the value of  $\epsilon_r$ . They both increase by about 2 GHz when  $\epsilon_r$  is varied from 3.0 to 5.0 at  $45^\circ$  incidence. The optimum fit to the measurements over our range of polyester thicknesses occurs when an effective value of 3.5 is adopted, although in Fig.3b the agreement would have been improved further with a slightly smaller value. There, the inner radii of the rings were 1.2 and 1.9 mm, with widths 0.3 mm. The H-plane performance limits the transmission mode bandwidth in dual linearly polarised oblique incidence diplexers. The band at 24 GHz in Fig.3b is about 10% wide to the -0.5 dB points.

LINEAR CROSSPOLAR PERFORMANCE IN A  $45^\circ$  INCIDENCE DIPLEXER

The four arrays with dimensions given in Fig.2 were used in turn as the plane dichroic surface in the diplexer sketched in Fig.1. The feeds at each frequency band were smooth walled horns with 10 dB beamwidths of about  $20^\circ$ , placed 9 cm from the array centres. Polarising grids were placed in the feed apertures. The arrays were 20 cm square and

TABLE 1 - Transmission and reflection bandwidths for 45° incidence

Array	Reflection	Common Bandwidth (GHz)	Band centre ratio
	Transmission		
Jerusalem cross	19.5 - 24.0 (21%)	32.0 - 35.0 (10%)	1.5
Concentric rings	16.5 - 19.0 (14%)	23.0 - 25.5 (10%)	1.4
Double squares	14.0 - 16.5 (16%)	21.5 - 24.2 (13%)	1.5
Gridded squares	22.4 - 26.3 (16%)	17.0 - 18.5 (8%)	1.4

were again printed on polyester substrates 0.021 mm or 0.134 mm thick. Each array was orientated so that one side of the lattice square was in the plane of incidence.

#### Copolar Bandwidths

The measured -0.5 dB bandwidths common to both principal planes of incidence are listed in Table 1 together with the ratios of band centre frequencies. All four arrays are capable of achieving reasonable bandwidths ( $\geq 8\%$ ) with small spacing ratios ( $\leq 1.5:1$ ). In transmission, the bandwidth of each array is determined mainly by the H-plane frequency response. This in particular limits the common band for the gridded square to 8%, although wider bands may perhaps be obtained with more careful choice of the grid dimensions. The widths in reflection are determined by the E-plane response and are greater than those obtained in transmission, varying from 14% for the concentric rings to 21% for the Jerusalem cross.

#### Crosspolar Levels

The peak linear crosspolar levels measured in the 45° planes in the copolar transmission and reflection bands are plotted in Fig.4. For the Jerusalem cross the levels range from -31.5 dB to -39.5 dB in reflection and from -26 dB to -35 dB in transmission, where the average levels increase steadily towards the low frequency edge of the band. On average the levels in reflection are 2 to 3 dB lower for E-plane incidence. The levels for the concentric ring array (Fig.4b) vary from -31.5 dB to -35.5 dB in reflection and from -32 dB to -37.5 dB in transmission, being again lower in the E-plane. In Fig.4c the average levels for the double squares are about -35 dB in reflection and -37 dB in transmission, with no appreciable difference for the two field orientations. For the gridded square the levels range from about -32 dB to about -39 dB in both bands. The repeatability of these levels was about  $\pm 1$  dB.

#### COINCIDENCE OF BAND CENTRES

The greater degree of depolarisation measured for the Jerusalem cross in transmission is associated partially with the lack of coincidence of the transmission band centres in the two principal planes of incidence. They differ by about 1.5 GHz, whereas for the other three arrays they are virtually coincident. The dependence of the crosspolarisation on the coincidence of bands in the principal planes is illustrated by the performance of three arrays of single rings in the diplexer system. The rings had inner radii of 1.2 mm in all three arrays and were arranged on square lattices (Fig.5). The E- and H-plane transmission curves are sketched in Fig.6a. Crosspolar levels measured in the 45° planes across the -0.5 dB copolar

reflection bandwidths are summarised in Fig. 6b.

For array 1, where the rings are relatively widely spaced with  $2r/D = 0.61$ , the reflection band centres differ by about 2 GHz and as a result the common bandwidth is limited to about 9%, from 32.5 to 35.5 GHz. The peak crosspolar levels vary from about -34 dB at 32.5 GHz to -24 dB at the upper edge of the band for E-plane incidence, while for H-plane incidence the levels are about 2 dB lower on average. Closer packing of the rings reduces the discrepancy between the measured reflection band centres. In array 2 for example, with  $2r/D = 0.64$ , the difference is now approximately 1 GHz and the bandwidth is 11%. The crosspolar levels are lower, varying from -37 dB at 30.5 GHz to -29 dB at 34 GHz, with an average of -31.5 dB. For array 3, where the rings are very closely packed,  $2r/D = 0.87$  and the band centres coincide. The common reflection bandwidth of 28% is now determined by that measured for the E-plane. The average of the peak crosspolar levels recorded between 27 and 34 GHz is now -35 dB, the levels then increasing to -30 dB at 36 GHz, the upper edge of the band. Fig.5 shows the clear improvement in crosspolar performance as the band centres become coincident.

#### CONCLUSIONS

These four elements are capable of giving close band spacings and reasonable bandwidths in 45° incidence dipoles. A criterion for levels of linear crosspolarisation well below -30 dB is the coincidence of band centres in the principal planes at oblique incidence.

#### ACKNOWLEDGEMENT

This work was supported by a research grant from the UK Science and Engineering Research Council.

#### REFERENCES

1. Arnaud, J.A., and Pelow, F.A., 1975, *Bell Syst. Tech. J.*, 54, 263-283.
2. Anderson, I., 1975, *Bell Syst. Tech. J.*, 54, 1725-1731.
3. Langley, R.J., and Drinkwater, A.J., 1982, *IEE Proc. H, Microwaves, Opt. & Antennas*, 129, 1-6.
4. Hamdy, S.M.A., Cahill, R., Langley, R.J., and Parker, E.A., 1982, "The Jerusalem cross and related structures in frequency selective surfaces", 8th Antenna Symposium, Queen Mary College, London.
5. Parker, E.A., Hamdy, S.M.A., and Langley, R.J., "Modes of resonance of the Jerusalem cross", *IEE Proc. H, Microwaves, Opt. & Antennas* (submitted for publication).

6. Parker, E.A., Hamdy, S.M.A., and Langley, R.J., 1981, Electron. Lett., 17, 880-881.  
 7. Amitay, N., Galindo, V., and Wu, C.P., 1972, "Theory and Analysis of Phased Array Antennas", Wiley, New York.

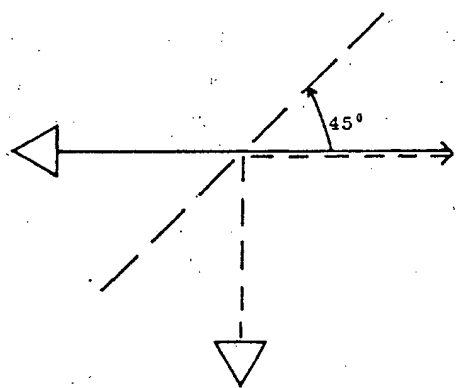


Figure 1  $45^\circ$  incidence diplexer

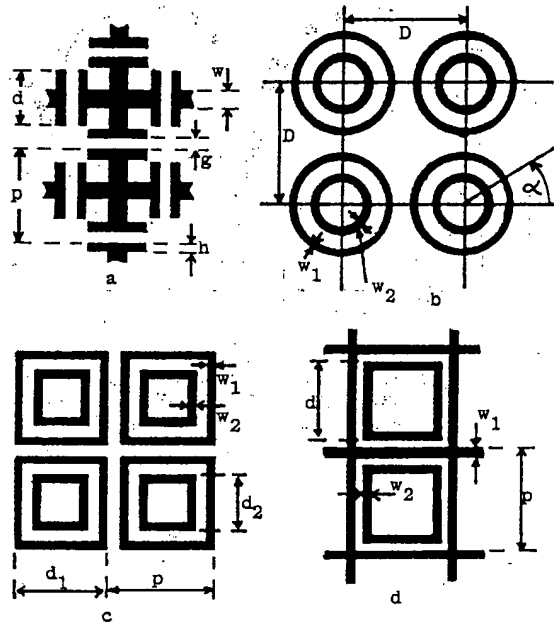


Figure 2 Dichroic array element geometries  
 (a) Jerusalem cross:  $p=4.0\text{mm}$ ,  $w=0.8\text{mm}$ ,  
 $d=2.6\text{mm}$ ,  $b=0.3\text{mm}$ ,  $g=0.3\text{mm}$

(b) Concentric rings: Outer ring mean radius 2.1mm. Inner ring mean radius 1.325mm.  $D=4.7\text{mm}$ ,  $w_1=0.2\text{mm}$ ,  $w_2=0.35\text{mm}$

(c) Double squares:  $p=5.0\text{mm}$ ,  $d_1=4.6\text{mm}$ ,  
 $d_2=2.9\text{mm}$ ,  $w_1=w_2=0.2\text{mm}$

(d) Gridded squares:  $p=4.5\text{mm}$ ,  $d=2.9\text{mm}$ ,  
 $w_1=0.3\text{mm}$ ,  $w_2=0.1\text{mm}$

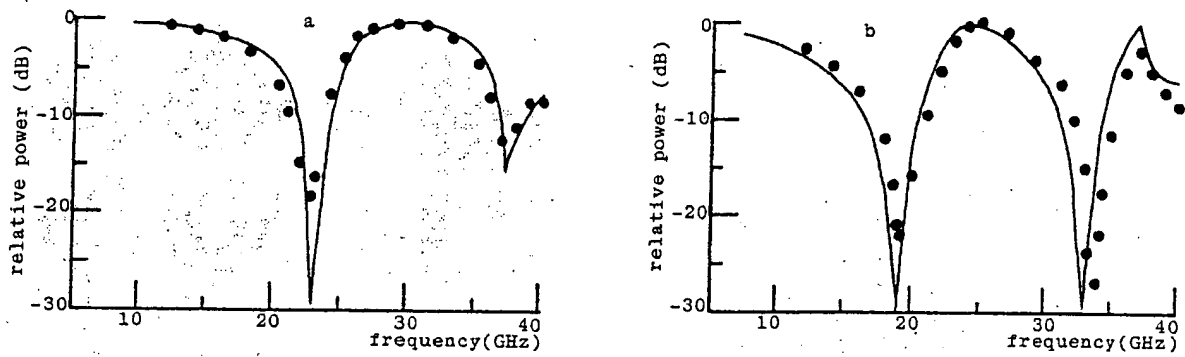


Figure 3 Plane wave transmission coefficients for concentric rings  
 (a) E-plane (substrate 0.021 mm thick).  
 Dots show measured values.  
 (b) H-plane (substrate 0.134 mm thick).

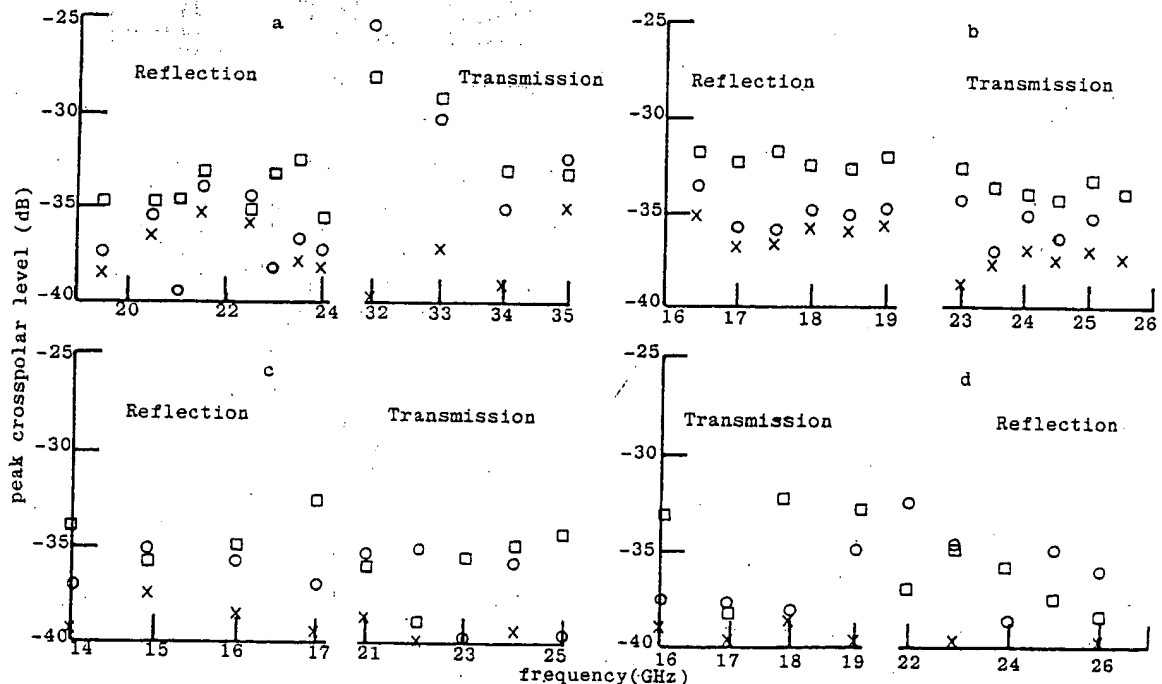
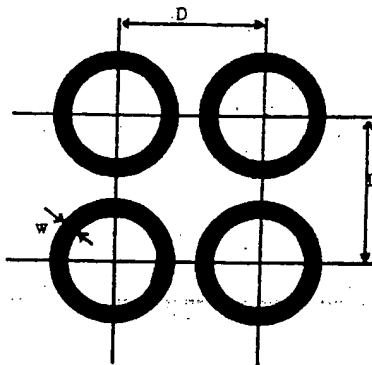


Figure 4 Peak crosspolar levels for: (a) Jerusalem cross array (b) Concentric ring array  
 (c) Double square array (d) Gridded square array. Squares: H-plane incidence  
 Circles: E-plane incidence Crosses: Feed without array



Array	D	w	$2r/D$
1	4.6	0.4	0.61
2	4.4	0.4	0.64
3	3.0	0.2	0.87

Figure 5 Simple ring array geometry  
 $r$  is the mean radius of the rings.  
Dimensions are in mm.

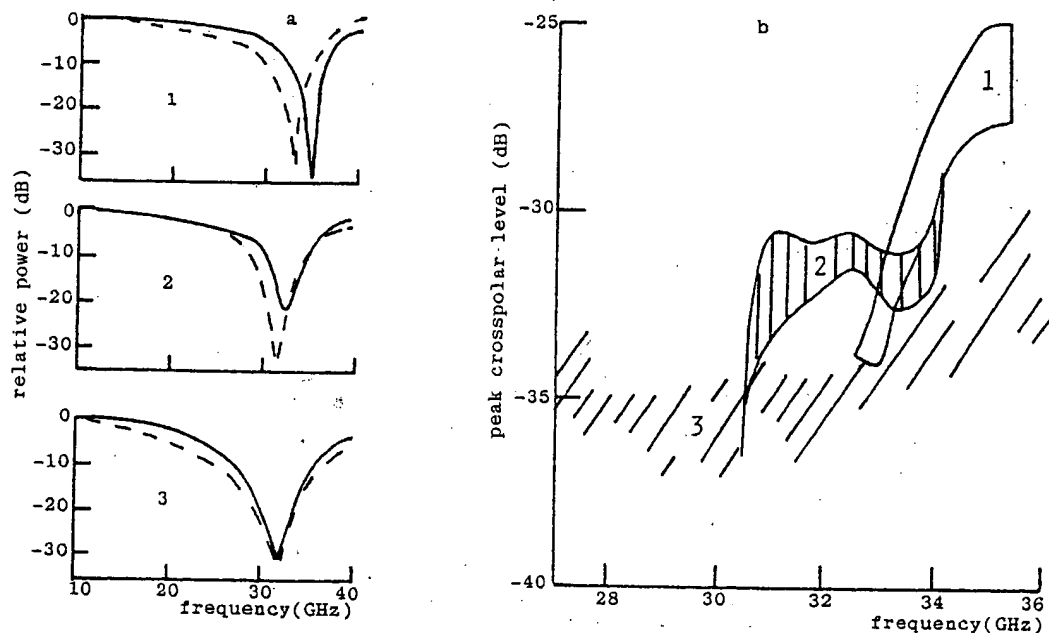


Figure 6 Measured responses for ring arrays 1-3. (a)  $45^\circ$ -plane transmission coefficients.  
E-plane incidence — H-plane incidence (b)  $45^\circ$ -plane crosspolar levels.  
Levels measured for both planes lie within regions shown